

Generation of squeezed light by intracavity frequency doubling

S. F. Pereira, Min Xiao, H. J. Kimble, and J. L. Hall*

Department of Physics, University of Texas at Austin, Austin, Texas 78712

(Received 13 July 1988)

Squeezed states of light are generated by the process of second-harmonic conversion within an optical cavity resonant at both fundamental and harmonic frequencies. Observations of squeezing are made by analyzing the spectral density of photocurrent fluctuations produced by the total field reflected from the nonlinear cavity. Reductions in photocurrent noise of 13% relative to the coherent-state or shot-noise level are achieved for frequency offsets near 4 MHz.

Recently squeezed states of light have been successfully generated in experiments involving a variety of physical processes.¹ While much of the research has concentrated on squeezing produced by four-wave mixing (either in atomic vapors or in condensed media), the most successful experiments have been those involving three-wave mixing in parametric down conversion.²⁻⁴ Given this large degree of squeezing generated via the second-order susceptibility, one naturally inquires about the use of frequency doubling for the production of squeezed states, for which an extensive theoretical literature is available.⁵⁻¹⁰ Of various possibilities, the scheme that we have chosen to investigate is that of second harmonic generation within an optical cavity resonant at both fundamental ω_L and harmonic $2\omega_L$ frequencies and driven by a coherent source at ω_L .⁷⁻¹⁰ In this Communication, we report observations of squeezing of the total fundamental field reflected from the nonlinear cavity. When this field illuminates a pair of photodiodes, we observe reductions in photocurrent fluctuations of 13% (-0.6 dB) relative to the coherent-state or shot-noise level for analysis frequencies around 4 MHz. We also identify a noise mechanism that has not been discussed for $\chi^{(2)}$ processes but which has had a significant impact on squeezed state production via $\chi^{(3)}$ in optical fibers.¹¹ Although our initial measurements show modest noise reductions below the coherent-state level, the results that we report are the first achieved with a process that has served as an important theoretical model for the investigation of quantum statistical processes in quantum optics.

The experimental arrangement that we employ is sketched in Fig. 1 and consists of a standing-wave cavity containing a crystal of lithium niobate doped with magnesium oxide (MgO:LiNbO_3) and driven by the field from a frequency-stabilized Nd:YAG (yttrium aluminum garnet) laser. The field reflected from the cavity illuminates a pair of high-quantum-efficiency photodiodes, whose individual photocurrents (i_a, i_b) are summed with either $0^\circ (+)$ or $180^\circ (-)$ phase difference to produce two photocurrents i_\pm . The spectral densities of the photocurrent fluctuations i_\pm are analyzed as functions of cavity detuning Δ_1 during the sweep of the cavity length through resonance of the fundamental field. An intensity regulator adjusts the incident light level during the scan to maintain an approximately constant low-frequency photocurrent I_a from one photodiode, thus eliminating the usual dip in

reflected power and providing a constant dc photocurrent as the backdrop in the search for squeezing.

Of course of principal importance in an experiment to detect squeezed states is the need to accurately determine the coherent-state noise level. As in the usual balanced homodyne detector, the photocurrent i_- (either in the presence or absence of nonlinear coupling within the cavity) provides a reference in our measurements for determining the coherent-state level, since for a properly balanced system excess local oscillator noise is greatly suppressed.^{12,13} For our detector arrangement, the suppression factor is greater than 20 dB over the frequency range of interest. Contrary to the usual implementation of the balanced homodyne detector in which the squeezed signal is delivered through the open port of the beamsplitter (BS in Fig. 1) and phase-sensitive signal fluctuations are reconstructed in the photocurrent i_- , the squeezed fluctuations in our experiment are encoded on the beam P_{r1} , which would normally be the local oscillator. Hence, squeezed fluctuations of the amplitude quadrature of P_{r1} are reconstructed in the photocurrent i_+ .¹⁴

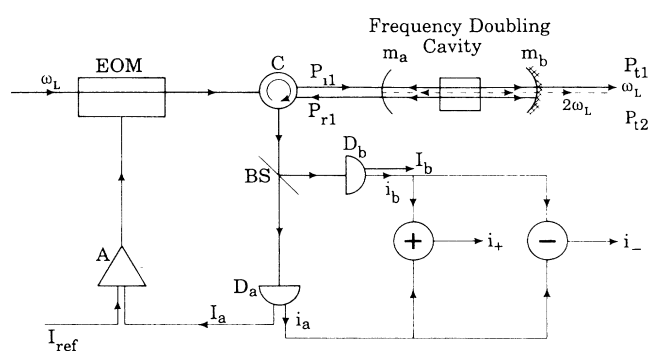


FIG. 1. Diagram of the principal elements in an experiment to generate squeezed states by intracavity frequency doubling. The cavity formed by mirrors (m_a, m_b) serves to convert the incident beam P_{i1} into a squeezed beam P_{r1} . The circulator C directs P_{r1} to a pair of photodiodes and associated amplifiers (D_a, D_b). (i_a, i_b) are the high-frequency ($\gtrsim 200$ kHz) components of the photocurrents while (I_a, I_b) are the low-frequency components. The current I_a can be held constant by a servo system consisting of amplifier A and electro-optic modulator (EOM).

Since any excess laser noise also appears in i_+ , our procedure of examining i_+ for noise reductions below the shot-noise level is valid only if the laser driving the cavity has no excess fluctuations above those of a coherent state. We have verified that this is indeed the case. Far from the cavity resonance ($\Delta_1 \gg 0$) the spectral densities of photocurrent fluctuations of i_+ and i_- coincide within $\pm 2\%$ over the entire range of frequencies quoted below.

Returning now to the question of the nonlinear optical processes responsible for generating squeezed states, we describe in more specific detail the relevant parameters of our experiment. The finesses of the cavity formed by mirrors (m_a, m_b) in Fig. 1 are $F_1 \approx 75$ and $F_2 \approx 45$, where throughout the subscript 1 (2) refers to the field at ω_L ($2\omega_L$). The transmission coefficients of m_a are ($T_{a1} = 0.058$, $T_{a2} = 10^{-5}$) while those of m_b are ($T_{b1} = 2 \times 10^{-3}$, $T_{b2} = 6 \times 10^{-4}$). The intracavity MgO:LiNbO₃ crystal is of length 25 mm; the cavity is operated in a near spherical configuration with mirrors of 100-mm radii. In the absence of servo control and of nonlinear intracavity conversion, the ratio of reflected fundamental power on resonance to that off resonance is approximately 0.4.

To make contact with the existing literature on the efficiency of the nonlinear conversion in our cavity, we consider the case of zero cavity detunings and no servo control of P_{i1} , for which the dimensionless fields $A \equiv$ (intracavity field at ω_L) and $B \equiv$ (incident field at ω_L) are related by^{7,9,14}

$$B^2 = A^2(1 + A^2)^2, \quad B^2 = (4F_1F_2\varepsilon_1E_{NL}P_{i1})/\pi^2, \quad (1)$$

while the power P_{i2} transmitted through m_b at $2\omega_L$ is

$$P_{i2} = (\pi^2 T_{b2} A^4) / (4F_1^2 E_{NL}). \quad (2)$$

Here ε_1 is the buildup factor for the incident power P_{i1} in the absence of harmonic conversion, while E_{NL} is the nonlinear conversion efficiency, the explicit form of which is given in Ref. 14. Note that implicit in the conversion efficiency E_{NL} is a particular constraint on the relative phases of the standing-wave patterns of the fundamental and harmonic modes within the crystal.^{14,15} In general, optimum conversion efficiency is not achieved for a standing-wave cavity even if both ω_L and $2\omega_L$ are simultaneously resonant within the cavity.

Over the range of incident power P_{i1} from 1 to 30 mW we have recorded the transmitted powers P_{i1} and P_{i2} and compared our measurements with the predictions of Eqs. (1) and (2). For the measured cavity parameters, we obtain reasonable quantitative agreement between theory and experiment for the dependence of P_{i2} and of A^2/B^2 on incident power P_{i1} if we view E_{NL} as a fitting parameter which is found to be $5 \times 10^{-4} \text{ W}^{-1}$ (note that A^2/B^2 gives the ratio of P_{i1} for $E_{NL} \neq 0$ to that for $E_{NL} = 0$). Since the theoretical maximum value of $E_{NL} \sim 5 \times 10^{-3} \text{ W}^{-1}$, the observed conversion efficiency is markedly low, a point to which we will return shortly. A representative observation is $P_{i2} = 31 \text{ } \mu\text{W}$ and $A^2/B^2 = 0.75$ for $P_{i1} = 16 \text{ mW}$. If we operate with the intent of coupling more light out of the cavity at $2\omega_L$ (to the detriment of the generation of squeezing at ω_L) we obtain $P_{i2} = 4 \text{ mW}$ for $P_{i1} = 15 \text{ mW}$ and $T_{b2} = 0.03$.¹⁶

Our observations of noise reductions below the coherent-state level for the reflected cavity field are documented in Figs. 2 and 3. Figure 2 displays the spectral density Φ_+ of noise in the photocurrent i_+ as the length of the cavity is swept with ω_L fixed and with the total dc photocurrent ($I_a + I_b$) held constant ($\pm 1\%$) with the intensity servo. Figure 2(a) displays for reference the noise level far from the cavity resonance; Fig. 2(b) is taken in the absence of harmonic conversion as the cavity is swept through a longitudinal-mode resonance at ω_L . Figure 2(c) is recorded with efficient generation of the green field at $0.53 \text{ } \mu\text{m}$ and exhibits noise reduction below the shot-noise level ($\Phi_+ = 0$). Here the spectral densities of photocurrent noise $\Phi_{\pm}(\nu, \Delta_1)$ are defined in terms of the rms current fluctuations $i_{\pm}(\nu, \Delta_1)$ at a particular analysis frequency ν and cavity detuning Δ_1 by $\Phi_{\pm}(\nu, \Delta_1) = 20 \log_{10}[i_{\pm}(\nu, \Delta_1)/i_{\pm}(\nu, \Delta_1 \gg 0)]$. In Fig. 2, the dashed line gives the shot-noise level as determined by the signal $i_{\pm}^2(\nu, \Delta_1 \gg 0)$, which is a level that coincides with $i_{\pm}^2(\nu, \Delta_1 \gg 0)$ to within $\pm 2\%$. Recall that amplitude fluctuations of the reflected cavity field are reconstructed in the photocurrent i_+ (and hence in Φ_+) while these fluc-

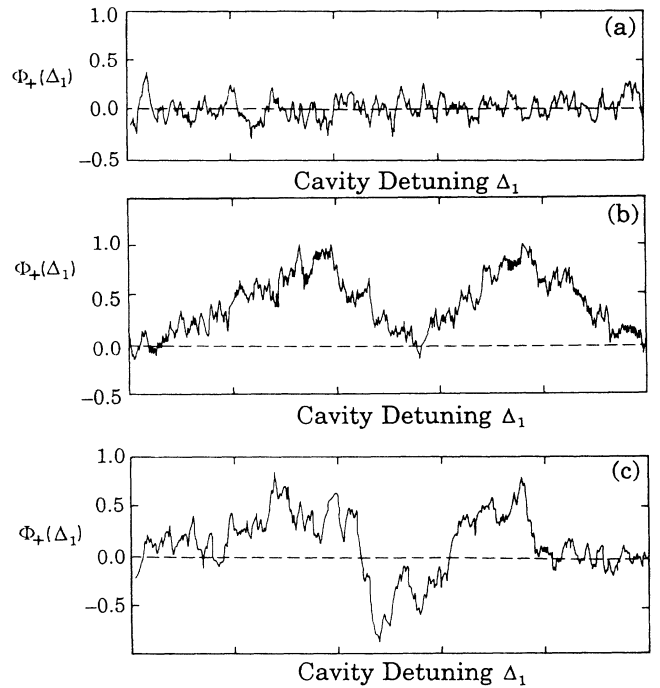


FIG. 2. Spectral density Φ_+ of photocurrent fluctuations i_+ as a function of cavity detuning Δ_1 of the fundamental field. The dashed line gives the shot-noise level. (a) Cavity detuned far from resonance. (b) Cavity swept through resonance in the absence of nonlinear conversion, with the peak of the cavity transmission occurring at the position of the central valley. (c) Cavity swept through resonance with nonlinear conversion resulting in the buildup of fields at both $(\omega_L, 2\omega_L)$. This trace gives evidence for noise reduction below the shot-noise level in the central region of the transmission profile. The analysis frequency in (a)–(c) is 2.5 MHz; analysis bandwidth equals 100 kHz. The incident power $P_i = 4 \text{ mW}$ for $\Delta_1 \gg 0$; the time for the entire sweep is 100 ms.

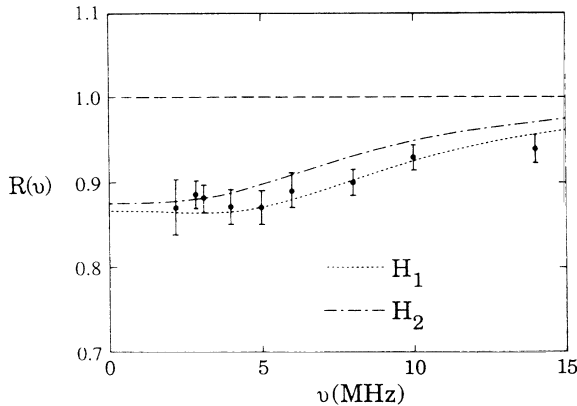


FIG. 3. Noise level $R \equiv 10^{0.1\Phi_+}$ as a function of analysis frequency ν (cycles/s). The dashed horizontal line at $R=1.0$ corresponds to the coherent-state level, with zero noise at $R=0$. Each data point is obtained from traces such as those shown in Fig. 2 with the error bars providing a rough estimate of uncertainty. The curves H_1, H_2 are obtained from the theory of Ref. 10 as discussed in the text, with H_1 drawn for $A^2=0.3$ and H_2 for $A^2=0.2$.

tuations are greatly suppressed in i_- (and hence in Φ_-). Indeed, the spectral density Φ_- exhibits no measurable detuning dependent noise variations as a function of Δ_1 . Furthermore, note that a coherent state should produce a flat, featureless noise spectrum Φ_+ as a function of cavity detuning at the level indicated by the dashed line in Fig. 2(b) with the intensity servo in operation. Instead, we observe an M -shaped noise feature as we sweep through the cavity resonance at ω_L [the position of the cavity transmission maximum is near the minimum of the valley in the noise spectrum and the width of the transmission profile is approximately that of the feature shown in Fig. 2(b)]. This excess noise above the coherent-state limit even in the absence of nonlinear conversion is due to classical phase modulation produced by thermal fluctuations in the refractive index of the intracavity doubling crystal. A simple model in which the index is driven through the photoelastic effect to produce (small) Gaussian fluctuations of the intracavity phase adequately describes the qualitative features of Fig. 2(b).^{11,14}

While these excess classical fluctuations associated with the intracavity medium are undesirable, they do not preclude the observation of squeezing. In the presence of intracavity harmonic generation, the trace in Fig. 2(c) indicates that the noise level drops below the shot-noise level ($\Phi_+=0$) at the position of the cavity resonance between the two regions of enhanced fluctuations. To pass from a trace such as in Fig. 2(b) without nonlinear coupling to a trace such as in Fig. 2(c) with nonlinear coupling we simply vary the servo-controlled temperature of the crystal to bring cavity modes at ω_L and $2\omega_L$ into approximate overlapping resonance somewhere under the phase matching curve resulting in efficient generation of the green field at $0.53 \mu\text{m}$ as the cavity is swept through resonance. From a collection of traces such as shown in Fig. 2, we infer noise reduction below the shot-noise level of (-0.6 ± 0.1) dB, corresponding to a drop of 13% below the coherent-state

limit. Although the data reported here are recorded by scanning the cavity detuning, we observe similar noise reductions by locking to the center of the cavity resonance at ω_L with a rf sideband technique to hold the detuning Δ_1 fixed near the position of the noise minimum. In either the swept detuning mode or the locked mode of data acquisition the largest degree of squeezing is not obtained coincident with the highest output P_{i2} at $2\omega_L$. Instead as the crystal temperature is scanned we consistently observe an initial decrease in noise below $\Phi_+=0$ as the green intensity grows, followed by an increase in noise to $\Phi_+ \sim 0$ near the point of maximum green generation, followed by another decrease in noise below $\Phi_+=0$ as the green intensity diminishes. At present, we have no satisfactory explanation for this behavior.

We explore the rf dependence of the noise reduction $R(\nu) = 10^{0.1\Phi_+(\nu)}$ in Fig. 3 in which each point is obtained by recording several traces such as those shown in Fig. 2 at fixed analysis frequency in the spectrum of photocurrent fluctuations. The total reflected power is again stabilized to $\pm 1\%$ for the measurement, with the incident power P_{i1} varying between 7 mW for $\Delta_1 \gg 0$ to value greater than $(7 \text{ mW} / D_0) = 18 \text{ mW}$ for $\Delta_1 = 0$. As a point of reference we include in Fig. 3 two theoretical curves obtained from Eq. (4.4) of Ref. 10 supplemented with the analysis presented in Ref. 14, Eq. (10). The curves are evaluated for parameters appropriate for the experiment; namely the ratio $f \equiv F_1/F_2 = 1.7$ and $A^2 = (0.2, 0.3)$, corresponding to $P_{i1}(\Delta_1 = 0) \approx (13 \text{ mW}, 22 \text{ mW})$ for $\Delta_1 = 0$. The overall propagation and detection efficiency ξ for the squeezed fluctuations includes the cavity escape efficiency (0.75), the transmission efficiency from cavity to photodetector (0.80), the detector quantum efficiency (0.83), and the homodyne efficiency for overlap of the direct reflection and the cavity leakage field (0.80), resulting in $\xi \approx 0.40$. From Fig. 3, we see that our observations of noise reduction are in reasonable qualitative agreement with theoretical estimates for our system. We stress that this agreement may be fortuitous since the theory of Ref. 10 assumes zero detuning for both ω_L and $2\omega_L$, while our experiments are conducted largely without knowledge of the relative detuning and without precise control of E_{NL} . The relatively low conversion efficiency and the large ratio of cavity loss rates are responsible for the absence in Fig. 3 of the distinctive spectral features predicted for $A^2 \sim (1+f)$ around the frequency ν_0 of the self-pulsing instability ($\nu_0 \sim 11 \text{ MHz}$ for our system with a threshold $P_{i1} \sim 1.6 \text{ W}$ for zero detunings).^{10,14}

Several comments should be made regarding the prospects for improving these initial observations. In the first place, the intracavity losses at $2\omega_L$ can be substantially reduced with improved coatings of the intracavity optics. Secondly, E_{NL} can be greatly increased by adding degrees of freedom to our apparatus to allow optimization of the coupling integral of cavity modes at ω_L and $2\omega_L$ and control of the position of simultaneous resonance with respect to the phase matching curve. These improvements would result in a greatly reduced threshold for self-oscillation and in a greater role for nonlinear processes relative to the classical phase noise produced in the cavity. Additionally, substantially increased degrees of squeezing are predicted

for reduced values of f .

In summary, we have employed the process of intracavity frequency doubling to generate a squeezed beam of light by reflection of a laser from a nonlinear cavity. Noise reductions of 13% relative to the coherent-state or shot-noise level have been observed. Thermally driven fluctuations in the index of refraction of the intracavity doubling crystal lead to phase noise that complicates the investigation of squeezing. The issue of the interplay of

the classical phase noise with the nonlinear conversion is one that we are currently addressing theoretically.

This work was supported by the Office of Naval Research Grant No. N00014-87-K-0156 and by the Venture Research Unit of British Petroleum America. One of us (S.P.) acknowledges support from Coordenação de Aperfeiçoamento de Pessoal do Ensino Superior (CAPES), a Brazilian Institution.

*Permanent address: Joint Institute for Laboratory Astrophysics, National Bureau of Standards and University of Colorado, Boulder, CO.

¹*Squeezed States of the Electromagnetic Field*, edited by H. J. Kimble and D. F. Walls [J. Opt. Soc. Am. B **4**, 1450–1741 (1987)].

²L. A. Wu, H. J. Kimble, J. L. Hall, and H. Wu, Phys. Rev. Lett. **57**, 2520 (1986).

³A. Heidmann, R. J. Horowicz, S. Reynaud, E. Giacobino, and C. Fabre, Phys. Rev. Lett. **59**, 2555 (1987).

⁴P. Grangier, R. E. Slusher, B. Yurke, and L. LaPorta, Phys. Rev. Lett. **59**, 2153 (1987).

⁵L. Mandel, Opt. Commun. **42**, 437 (1982).

⁶S. Kielich, R. Tanaš, and R. Zawodny, J. Mod. Opt. **34**, 979 (1987).

⁷P. D. Drummond, K. J. McNeil, and D. F. Walls, Opt. Acta **27**,

321 (1980); **28**, 211 (1981).

⁸G. J. Milburn and D. F. Walls, Phys. Rev. A **27**, 392 (1983).

⁹L. A. Lugiato, G. Strini, and F. De Martini, Opt. Lett. **8**, 256 (1983).

¹⁰M. J. Collett and D. F. Walls, Phys. Rev. A **32**, 2887 (1985).

¹¹R. M. Shelby, M. D. Levenson, S. H. Perlmuter, R. G. DeVoe, and D. F. Walls, Phys. Rev. Lett. **57**, 691 (1986).

¹²H. P. Yuen and V. W. S. Chan, Opt. Lett. **8**, 177 (1983).

¹³L. A. Wu, Min Xiao, and H. J. Kimble, J. Opt. Soc. Am. B **4**, 1465 (1987).

¹⁴H. J. Kimble and J. L. Hall, in *Quantum Optics IV*, edited by J. D. Harvey and D. F. Walls (Springer-Verlag, Berlin, 1986), pp. 58–69.

¹⁵L. A. Wu and H. J. Kimble, J. Opt. Soc. Am. B **2**, 697 (1985).

¹⁶W. J. Kozlovsky, C. D. Nabors, and R. L. Byer, J. Quant. Electron. **24**, 913 (1986).